Journal of Alloys and Compounds 509 (2011) 5748–5754

Contents lists available at ScienceDirect

Journal of Alloys and Compounds

journal homepage: www.elsevier.com/locate/jallcom

Continuous control as alternative route for wear monitoring by measuring penetration depth during linear reciprocating sliding of Ti6Al4V alloy

F. Zivic[a,*], M. Babic[a], S.Mitrovic[a], A. Vencl[b]

[a] Tribology Laboratory, Faculty of Mechanical Engineering, Kragujevac, Serbia
[b] Tribology Laboratory, Faculty of Mechanical Engineering, Belgrade, Serbia

ARTICLE INFO

Article history:
Received 17 November 2010
Received in revised form 23 February 2011
Accepted 27 February 2011
Available online 5 March 2011

Keywords:
Titanium
Alumina
Wear
Biomaterials
Penetration depth

ABSTRACT

Continuous wear monitoring during linear reciprocating sliding was investigated. Tribological tests with Ti6Al4V alloy against alumina, at nanotribometer, on microscale, were realised in dry conditions over a range of loads (100–1000 mN) and velocities (4–12 mm/s). Wear factors were calculated, for each conducted test, in two different ways. Wear factors calculated according to observed geometry of the worn tracks (according to ASTM G133 standard) were compared to values calculated according to penetration depth parameter continuously recorded by nanotribometer and results were highly correlated. Penetration depth curves and wear factor curves were obtained and analysed. Wear mechanisms based on examinations of worn surfaces by optical microscopy, were analysed in comparison with trends of penetration depth curves. Development of wear mechanism over time was further investigated. The obtained results showed that the wear factor values are strongly influenced by the applied load.

1. Introduction

Wear measurements in tribological testing usually involve measurements of mass loss or a worn track dimension after experiment is finished. Wear amount can be described in terms of mass loss (g), linear dimensional change (mm) or volume loss (mm^3). The mass loss of observed triboelement can be determined by weighing it before and after tribological testing. It gives information about final wear amount. Volume loss of the sample can be calculated after the test, by measuring wear track length and average cross-sectional area of the wear track, using optical microscopy. Volume loss of the sample can also be derived from the mass loss. Continuous wear monitoring can be realised by interrupting tribological test to perform wear measurements at certain periodic time intervals [1–3]. However, these procedures can influence testing due to necessary removing, cleaning and measuring of the samples. It is also time consuming process. For instance, measurement of the mass loss requires the test to be stopped and the sample removed for weighing.

There is a need to continuously monitor wear during sliding in many applications where development of wear mechanisms are important to control and predict, such as in case of biomedical implants [4]. It is important to simulate development of wear process and to distinguish changes in wear mechanisms during the motion of articulating surfaces. Very low wear rates are present in modern tribological systems, such as in case of hip joint tribo-system (wear rates of order of 10^{-7} mm^3/Nm). Precise measurements of mass loss in such cases involve sophisticated and expensive equipment and still needs more reliable solutions in many real applications. It is, therefore, especially important to continuously monitor change of the wear level at microscale.

Long and Rack [4] used ultrasonic pulse-echo technique for continuous wear measurement of orthopaedic titanium alloys. They showed that changes of the length loss parameter (dimensional change) can be used as a parameter indicating wear rate. Meozzi [5] validated a procedure for analysis of the wear behaviour (continuous wear monitoring) during sliding on the basis of geometrical experimental variables of the contact pair (ball and disc). Baets et al. [6], showed that continuous measurement of the normal approach of samples during relative contact can be used to obtain wear curves separately for both contact materials. They developed mathematical wear model by which normal approach measurements can be converted to wear volume curves (ball-on-flat type of contact). Since nanotribometer records penetration depth parameter during sliding, as a variable related to normal approach between surfaces in relative contact, it is possible to use it for continuous wear monitoring.

Total hip replacement using an alumina (Al_2O_3) head and socket and titanium alloy stem have been used for years in medical practice. Problems in relation to prosthetic failure still represent the major clinical problem for hip replacement, where the wear of materials in contact is the dominant reason leading to revision

* Corresponding author.
E-mail address: zivic@kg.ac.rs (F. Zivic).

0925-8388/$ – see front matter © 2011 Elsevier B.V. All rights reserved.
doi:10.1016/j.jallcom.2011.02.158

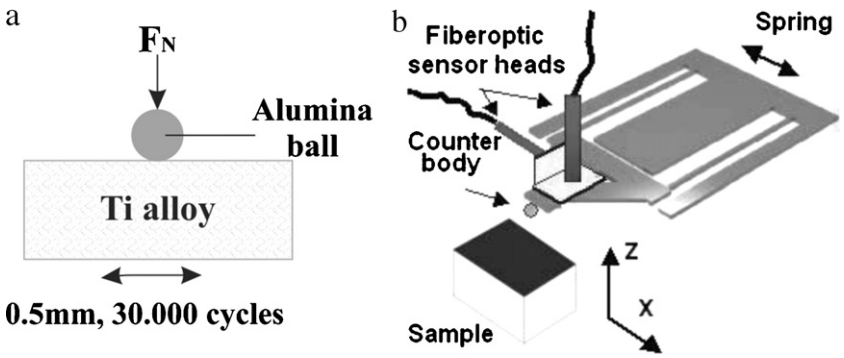

Fig. 1. Nanotribometer: (a) contact geometry; (b) linear reciprocating module.

surgeries. Titanium alloys are extensively used as biomaterials [7,8] due to their excellent properties such as biocompatibility and low density (4.5 g/cm^3). Development of advanced biomaterials is aimed toward creating biomaterials with properties such as Young's modulus close to that of the bone (approximately 30 GPa). Elastic modulus of titanium based materials vary from 55 GPa (Ti–29Nb–13Ta–7.1Zr alloy) to 112 GPa (Ti6Al4V alloy) [8], what is lower compared to 316L stainless steel (210 GPa). Titanium based materials are often used for joints (e.g. femoral stem in hip replacements). Alumina is also commonly used as a biomaterial due to high strength, and stability in physiological environments [8].

The paper presents continuous wear measurement at microscale, during linear reciprocating sliding of Ti6Al4V alloy against alumina. Wear was measured by two approaches: standard method according to ASTM G133 standard and secondly using penetration depth parameter recorded by the nanotribometer. Analysis of wear mechanisms was realised, based on obtained changes of the wear factor.

2. Materials and experimental methods

2.1. Materials

The investigated material was extra-low interstitial (ELI) grade Ti6Al4V alloy, industrially produced by Krupp VDM GmbH, Germany, in the form of a bar, 38 mm in diameter. Flat Ti6Al4V alloy samples were cut from alloy bars (6.35 mm × 15.75 mm × 10.16 mm in size). Cut samples were mechanically grounded using 400–1000 grit papers and polished using 3 μm diamond suspension to metallographic quality. After that, they were annealed at 1000 °C for 1 h in Ar atmosphere and cooled in the furnace to the room temperature. Thermal treatment of the samples was performed in order to obtain a better performance of standard Ti6Al4V alloy due to change in microstructure, as described in more detail in [22]. Samples were again mechanically grounded with SiC paper (1200 grit) and cleaned for 30 min in an ultrasonic bath with ethyl alcohol, producing initial roughness of Ra = 0.3 μm. Finally, samples were polished by diamond paste on abrading wheel. Final roughness prior to testing was Ra = 0.07 μm. After that, Ti alloy samples were prepared for testing in accordance with ASTM F86. The surface of the samples was cleaned by ethyl alcohol using a soft cotton cloth, to minimize foreign material. Then, samples were immersed in isopropyl alcohol for 60 min, in order to remove any remaining surface contaminants. After that, samples were ultrasonically cleaned in distilled water for 60 min, and dried in hot-air dryer. They were stored in a desiccator, prior to testing. Commercial alumina (Al_2O_3) ball of 1.5 mm diameter was used as the other material in contact. Alumina has significantly higher hardness than the titanium alloy and deformation processes during sliding can be, in this case, assigned only to Ti6Al4V alloy.

2.2. Tribological tests

Tribological tests were realised on the CSM Nanotribometer and linear reciprocating sliding mode was used. Static body was 1.5 mm diameter alumina ball. Moving body was flat rectangular Ti6Al4V alloy sample. Schematic diagram of the contact geometry and linear reciprocating module of the tribometer is shown in Fig. 1. Testing was done with 0.5 mm stroke (0.25 mm half amplitude) in dry conditions, in ambient air (temperature of 25 °C). Five values of normal force were selected (100 mN, 250 mN, 500 mN, 750 mN, 1000 mN) and three values of sliding speed (4 mm/s, 8 mm/s, 12 mm/s). The values of estimated maximum contact pressure are 0.68, 0.93, 1.17, 1.34 and 1.47 GPa, respectively. Duration of one test was 30,000 cycles, whereat distance of two strokes represents one cycle. Selected sliding velocities corresponds to the range of speed characteristic for hip joints testing (0–50 mm/s) [9].

Nanotribometer can continuously measure penetration depth (PD) parameter. Penetration depth parameter describes the depth to which alumina ball penetrates the flat surface of the Ti6Al4V sample during sliding, thus determining depth of the wear track on the flat sample.

Nanotribometer is equipped with optical displacement sensor (fiberoptic sensors) for measuring deflection of the cantilever (Fig. 1b), with high sensitivity. Light emitted from the sensor tip is reflected from the surface of the cantilever, received by the sensor and converted into electrical signal. The signal is related to the distance between the sensor tip and a reflective area on the cantilever. Due to a nature of fiberoptic sensors, besides measuring forces, it is also used to measure distance between the cantilever tip (tip of the alumina ball) and flat surface of the sample (Ti alloy), which represents penetration depth parameter. PD values are recorded as dynamic values during sliding, representing current position of the alumina ball in relation to the flat Ti sample (in μm), after observed number of cycles (or sliding distance).

Wear volume of the flat Ti alloy sample was calculated after each finished test, by measuring wear track width and length using optical microscopy (OM), according to ASTM G133. Wear of the ball was neglected since the surface of the alumina ball that was in contact exhibited only changes of the color, but without dimensional change, what was confirmed by OM. Wear volume, V, was calculated using obtained length of the wear track and average cross-sectional area of the worn track. Assumption was made that the cross-sectional area is a flat segment of a sphere corresponding to geometry of the alumina ball.

Wear factor, i.e. a specific wear rate parameter, k was calculated according to the following equation [10]:

$$k = \frac{V}{Fs}[\mathrm{mm^3/Nm}] \quad (1)$$

where F is the normal load, s, the total sliding distance, V, the wear volume at the end of the test.

Parallel to the previous procedure, calculation of the wear factor, k_{PD}, was done by another method. Wear factor, k, and wear factor, k_{PD} specify the same direct wear quantities, whereat k denotes the wear factor calculated using geometrical dimensions of the worn track by OM after the finished wear test and k_{PD} denotes wear factor calculated using PD parameter value at the end of the test, provided by nanotribometer. Wear volume, V_{PD} of the flat sample, at the end of the test, was calculated using maximum penetration depth (PD) parameter recorded by nanotribometer, after simple geometrical calculation. It was assumed that the cross-sectional area is a flat segment of a sphere, with PD representing height of that flat segment. Wear factor, k_{PD}, was calculated according to the following equation:

$$k_{PD} = \frac{V_{PD}}{Fs}[\mathrm{mm^3/Nm}] \quad (2)$$

Results of the wear factor calculated in two ways, once using standard geometrical approximation and secondly using PD parameter was compared. It was done in order to determine whether it is suitable to use continuously recorded values of PD parameter for continuous wear monitoring of the Ti6Al4V sample during sliding.

Continuously recorded PD values over time, during one test, provided as raw data by nanotribometer software, enabled calculation of wear factor values, k_t, continuously during testing. Wear factor curves as a function of the sliding distance, during the test, were obtained by simple mathematical processing of raw PD data, according to equation (3), analogue to the previous equation (2), and presented as diagrams further in the text:

$$k_t = \frac{V_t}{Fs_t}[\mathrm{mm^3/Nm}] \quad (3)$$

where, F is the normal load, s_t, the sliding distance after time t, V_t, the wear volume after sliding distance s_t.

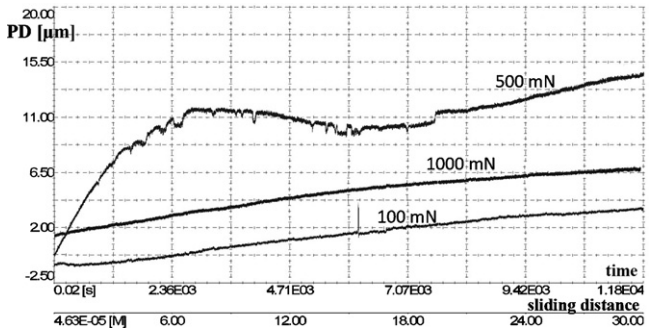

Fig. 2. Penetration depth (PD) curve, (4 mm/s); (a) 100 mN, (b) 500 mN, and (c) 1000 mN.

3. Results

Selected penetration depth curves over the sliding distance, as recorded by nanotribometer, during the contact, at 4 mm/s, are shown in Fig. 2. Generally, diagrams in Fig. 2 suggest that sample exhibit significantly different PD parameter behaviour over time, depending on applied normal load. In case of 100 mN, maximum PD value was below 3.5 μm and PD curve has a trend of continuously rising over time. In case of 1000 mN, maximum PD value is below 6.5 μm and also has a rising trend over the whole sliding distance. PD curve in case of 500 mN is different compared to other two cases (100 mN, 1000 mN). Normal load of 500 mN produce PD values significantly higher, up to 15 μm and also exhibited other shape of the PD curve. Maximum PD values are low for the lowest applied load of 100 mN and increase significantly with load increase, then after 500 mN it decreases again. Trends of the penetration depth curves in relation to 250 mN and 750 mN loads are similar to the one of 100 mN and 500 mN load respectively.

OM photographs of the worn surfaces on cleaned Ti alloy sample after sliding at 4 mm/s under different applied loads, corresponding to PD plots in Fig. 2, are presented in Fig. 3. It can be clearly seen that different wear mechanisms governed the sliding process, depending on the normal load. In case of 100 mN (Fig. 3a), evidence of mixed influence of tribochemical wear, abrasive wear and adhesion can be noticed (denoted by TH, G and A in Fig. 3). Worn track in Fig. 3b indicated that abrasive wear is dominant since only small regions of the worn track were subjected to adhesion and tribooxidation. Almost smooth and shiny worn track was produced during the sliding at 500 mN (Fig. 3b). Grooves and scratches are clearly seen and surface appeared as polished compared to other load regimes. In case of 1000 mN (Fig. 3c) area of displaced

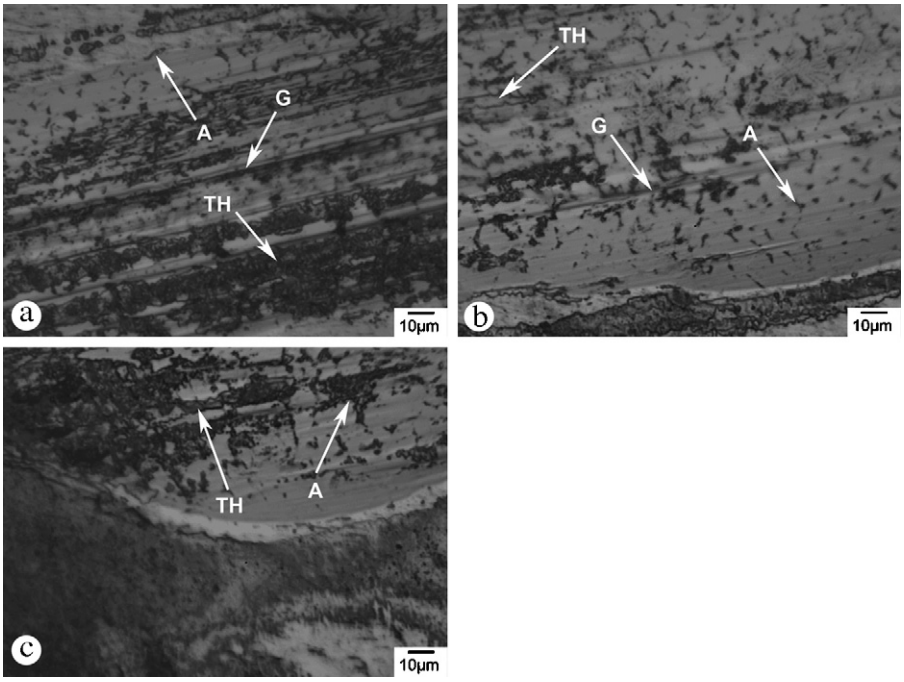

Fig. 3. Wear tracks on Ti alloy sample (4 mm/s): (a) 100 mN, (b) 500 mN, and (c) 1000 mN (A – adhesive wear; TH – tribochemical wear; G – groove).

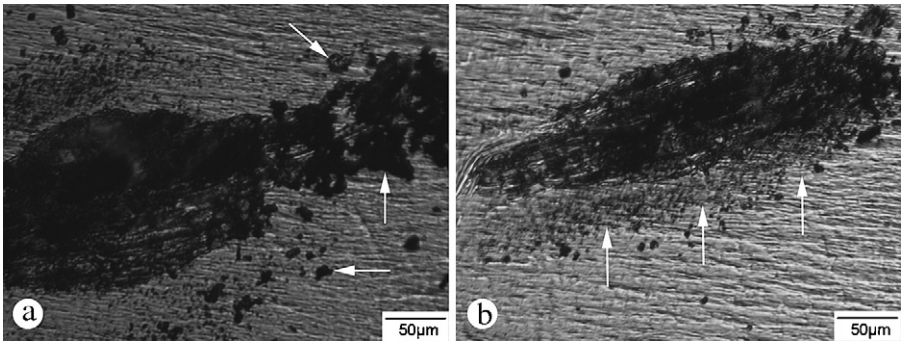

Fig. 4. Wear track, (4 mm/s): (a) 500 mN, (b) 1000 mN.

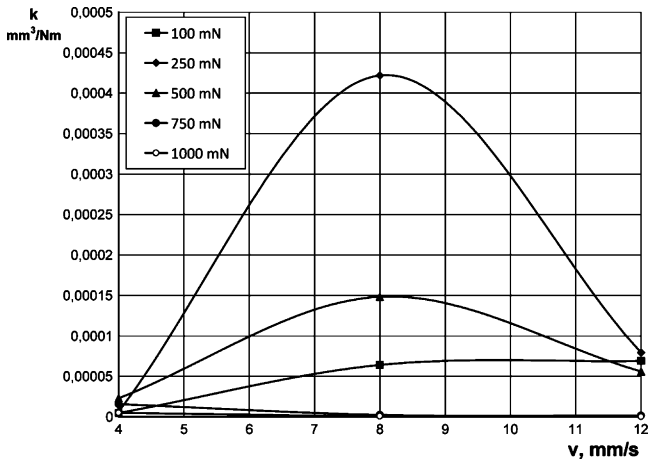

Fig. 5. Wear factor: sliding speed and normal load dependency.

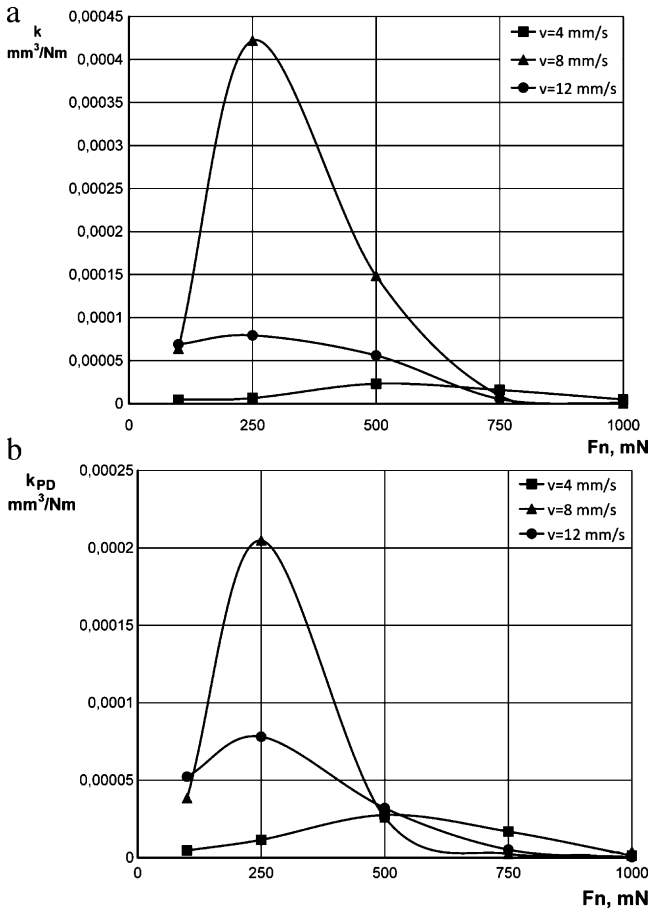

Fig. 6. Comparison of wear factors k and k_{PD}. (a) $v = 4$ mm/s; (b) $v = 8$ mm/s; (c) $v = 12$ mm/s;.

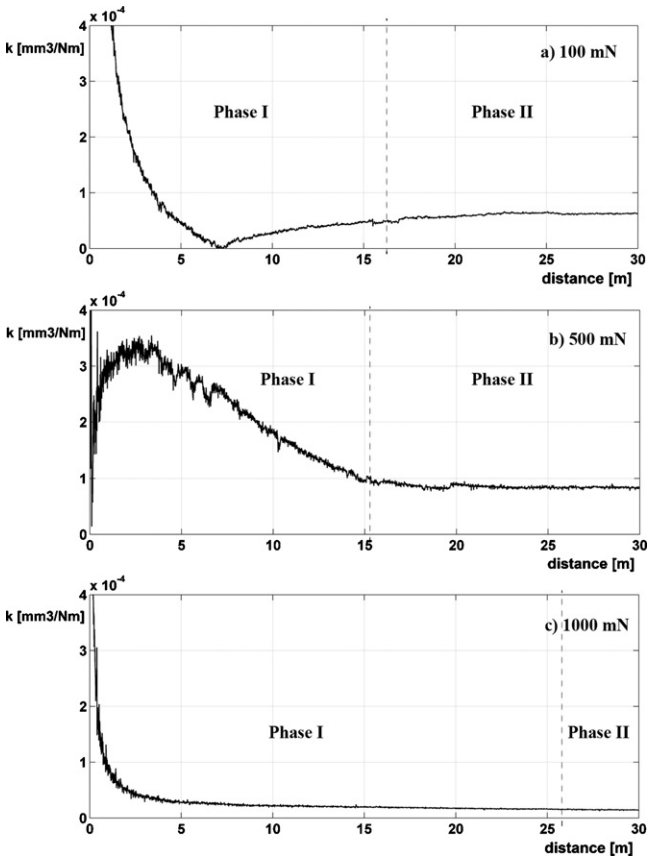

Fig. 7. Wear factor curve, (4 mm/s); (a) 100 mN, (b) 500 mN, and (c) 1000 mN.

surface (formed ridges) along the edge of the wear track can be noticed, indicating more intensive adhesive wear than in case of 100 mN. Also, evidence of tribochemical and abrasive wear can be observed in case of 1000 mN. Tribochemical wear was observed throughout the wear tracks by OM, as regions with rusted appearance (green and yellow colored regions) and they are denoted by TH in Fig. 3. Areas of adhesive wear in the wear track are denoted by A in Fig. 3 (number of small black regions). Other authors who studied wear behaviour of Ti6Al4V alloy [11,12,14], proved that the chemical reaction between Ti6Al4V and Al_2O_3 and tribooxidation on Ti6Al4V surface influence the wear process causing mild tribochemical wear during sliding. Worn surfaces in Fig. 3a and c are similar in appearance, and similar wear factor values were obtained for these conditions, as well.

Worn tracks on Ti alloy samples (with wear debris covering the track) after sliding at 4 mm/s under 500 mN and 1000 mN load, are presented in Fig. 4. It can be clearly seen that in case of 500 mN, coarse black wear debris, in form of clusters (denoted by arrows in Fig. 4a), is covering the track and that it is also accumulated at the leading edge of the track. Such a wear debris was produced only in case of 250 mN, 500 mN and 750 mN, but at the largest extent in case of 500 mN (Fig. 4a). It is obvious that the influence of the wear debris as the third body in the contact zone must be considered. In case of the lowest load (100 mN) wear debris was not accumulated in such clusters and was present in much smaller extent. Under the highest applied load (Fig. 4b) fine wear debris was distributed evenly throughout the worn track (denoted by arrows in Fig. 4b), not like in case of 500 mN.

4. Discussion

The variation of the wear factor, k, as functions of the sliding speed and load is illustrated in Figs. 5 and 6. Sliding speed showed no significant influence on wear behaviour of the observed Ti alloy, for the highest load applied (Fig. 5) and it exhibited transition characteristic for lower loads. The most pronounced transition was observed in case of 250 mN load. Change of the wear factor with applied normal force showed transition features for all observed speeds (Fig. 6). Wear level was the lowest for 1000 mN and the highest for normal loads of 250 mN and 500 mN.

Comparison of wear factors, k and k_{PD}, at 4 mm/s, 8 mm/s and 12 mm/s is presented in Fig. 6. It can be clearly seen that k and k_{PD} values are correlated to each other. Larger difference of k and k_{PD} values was obtained only for regimes under 8 mm/s speed (250 mN and 500 mN load). Similar results were obtained for all experimental conditions.

Wear factor curve as a function of the sliding distance, during sliding at 4 mm/s, under different loads, is presented in Fig. 7. Similar results were obtained for sliding speeds of 8 mm/s and 12 mm/s. It can be noticed that wear rate is changing during the test. Wear rate is the highest at the beginning of the test, during the running-in phase. Calculated maximum current values of the wear factor, k_t, at the beginning of the test, was 0.045 mm^3/Nm, 0.001 mm^3/Nm and 0.007 mm^3/Nm, respectively for 100 mN, 500 mN and 1000 mN load values (not shown in Fig. 7). The running-in period lasted approximately up to 1–2 m sliding distance, or 1000–2000 cycles of the test, depending on the applied load. In all conditions, steady state value was reached. It can also be noticed that the trend of the wear factor curve is different for different normal loads.

According to diagrams in Fig. 7, in all three cases of observed load, the testing can be divided into two phases: the first period exhibits significant changes of the wear factor, followed by the second phase when wear factor values can be described as rather constant (steady wear phase). In case of 100 mN load, during the first phase, wear rate is constantly decreasing until very low value is reached (0.9×10^{-6} mm^3/Nm), approximately after 7.5 m sliding distance (Fig. 7a). After that, wear rate again slowly increased until 17 m sliding distance, when it reached a wear factor value of approximately 0.6×10^{-4} mm^3/Nm, which stays constant until the end of the test (steady wear phase). In case of 500 mN load, (Fig. 7b), after very high initial values, wear factor abruptly decreased to 0.1×10^{-4} mm^3/Nm, then rapidly increased again, reaching 3.5×10^{-4} mm^3/Nm after approximately 3.5 m, and then it start decreasing again. After 15 m sliding distance it reaches its steady state value around 0.9×10^{-4} mm^3/Nm, and stays constant until the end of the test. In case of 1000 mN load, (Fig. 7c), wear factor curve is constantly decreasing throughout the test. It reaches its steady state value, around 0.15×10^{-4} mm^3/Nm, after approximately 26 m sliding distance, without sudden changes of the wear factor.

The obtained results showed that the wear factor values are strongly influenced by the applied load. Globally observed, load dependence exhibited transition feature, what is in consistence with findings of other authors [11,12]. However, sliding speed showed transition feature only for some load regimes (100 mN, 250 mN, 500 mN) and for other it had no significant influence on the wear factor. Dong and Bell [11], demonstrated transition characteristic of the sliding speed under all conditions. Different results obtained within this study in relation to sliding speed can be assigned to smaller range observed in this study. Dong and Bell [11] conducted tests over a higher range of speeds (0.0625–1 m/s). It is probable that sliding speed would show transition for all conditions here, if range is further increased. Load dependence transition characteristic can be clearly seen in Fig. 3. Wear level is increasing with load increase up to 250 mN or 500 mN and then with further load increase it rapidly decreases. This difference in wear rates can also be clearly seen if appropriate diagrams in Fig. 7 (steady state values) are compared.

Wear factors, calculated at the end of the test, indicate overall wear level for surfaces in contact, but do not imply anything about the change of the wear rate during the testing. Wear factors k and k_{PD}, calculated at the end of the test showed that they are correlated to each other, what can be clearly seen in Fig. 6. Consequently, wear related parameters calculated using continuously recorded PD parameter, can be used to describe wear behaviour during testing. Results of other authors who studied different techniques and methods for continuous wear measurement [4–6], indicated that experimentally obtained geometrical parameters can be used as additional mean for wear monitoring. It should be noted that fiberoptic sensors at nanotribometer due to their nature can measure the distance between the ball and the flat surface of the sample without interfering with the contact process itself.

It can be clearly seen that wear factor curves, as a function of the sliding distance during one test, as shown in Fig. 7, indicate different zones of wear behaviour. PD curves presented in Fig. 2, also indicate different behaviour of the contact pair, depending on the applied load, what is in consistence with findings of other authors [11,14]. Wear factor curve indicate mild steady state wear in case of 100 mN (Fig. 7a). This is in accordance with results obtained by Qu et al. [13] who reported wear factor of 5.7×10^{-4} mm^3/Nm, at 0.3 mm/s sliding speed (unidirectional sliding tests using pin-on-disk configuration), for wear of Ti6Al4V disks sliding against alumina. Dong and Bell [11] and Molinari et al. [12] proved that mild adhesive wear mechanism, accompanied by low tribochemical wear, is dominant for low load values. Since surface plot in Fig. 7a exhibits no significant sudden changes of the wear factor in its steady state and PD curve has constantly increasing trend, dominant wear mechanism do not change over time, for this load. When k factor change by a factor of 100 or even 1000 for a small change in conditions, it is usually associated with a change of predominant mechanism of material removal [10,21]. In case of 1000 mN load, wear factor curve in Fig. 7c also indicated low steady state wear factor. Since surface plot in Fig. 7c has general mildly decreasing trend without sudden increase or decrease in its steady state, no evidence of any changes of the dominant wear mechanism can be observed, as in the previous case of 100 mN. However, initial phases of wear factor curve in these two cases (100 mN, 1000 mN), both exhibited severe initial wear.

In case of 500 mN, PD curve (Fig. 2) and wear factor curve (Fig. 7b) has different appearance, compared to previous two cases, indicating significant changes in wear mechanism over time. If 250 mN and 750 mN load cases are considered, they showed less pronounced changes of the wear factor, and exhibited trend similar to the one under 500 mN. Surface plot in Fig. 7b indicated that during the first period of the test, very high wear rate occurred and penetration depth significantly increased also. It can be noticed that from 4 m to 7 m, PD curve has some sudden small decrease instantly followed by increase, and this is repeated along the line several times (Fig. 2). Simultaneously, wear factor values showed significant oscillations (Fig. 7b). Severe wear occurring at the beginning of the test, in case of 500 mN load (Fig. 7b), for a brief period, generated large quantities of the wear debris. Masmoudi et al. [1], proved that periodic ejection of particles layers occurred during sliding of Ti6Al4V against Al_2O_3, influencing wear rate values. They monitored tribological behaviour by stopping tests after certain predefined number of cycles and proved that different wear mechanisms were present during sliding under constant load and sliding speed. They observed dominant abrasive wear at the beginning phase, followed by adhesive wear up to some number of cycles when layers of wear debris particles were ejected away from the contact zone. After that, previous phases were repeated again periodically. Particle layers ejection was represented by sudden decrease and increase of the friction coefficient curve [1], and it is obviously comparable to sudden decrease and increase of PD curve observed in our study (Fig. 2). It is probable that during this period of sliding, layers of wear debris particles were ejected away from the contact zone.

From 10 m to 15 m of sliding distance, severe-to-mild wear transition can be clearly noticed (Fig. 7b). Specific wear factor k_t, changed by a factor of 3.5, even though there was no change in experimental conditions (load, velocity, environment), indicating

changes in wear mechanism. During this period, PD parameter is constant or decreasing showing approaching of surfaces in contact (500 mN load in Fig. 2). Period of severe-to-mild wear transition was probably governed by mixed influences of abrasive, adhesive and tribochemical wear, what is in accordance with findings of other authors [11,13]. During the period of steady state wear, penetration depth increased again, indicating mild abrasive wear.

Obtained PD curves (Fig. 2) were qualitatively compared with observed worn tracks after sliding (Figs. 3 and 4), under the same experimental conditions. It can be clearly seen (Fig. 4a), that wear debris is distributed at some distance around the wear track (indicated by arrows), showing that ejection of particles occurred, away from the contact zone. It is likely that wear debris, if present in larger extent within a contact zone, as shown in Fig. 4a, significantly contributed to increase of wear factor (Fig. 7b) more than three times if compared to the case of 1000 mN (Fig. 7c). According to our study, coarse wear debris clusters (Fig. 4a) indicated severe abrasive wear and implied that effect of the third body abrasion by these worn particles must be taken into account. This is in accordance with findings of several authors [11,12,14] who proved that tribochemical reaction between Ti alloy and alumina during sliding, has significant influence on the wear behaviour. Some authors [11,12], found that the major influence of the wear debris chemical composition can probably be assigned to titanium–aluminium intermetallic compounds (Ti_2Al_3, Al_3Ti) produced during sliding of Ti alloy against Al_2O_3. Dong and Bell [11] proved that Ti_2Al_3 particles appear during sliding. Since they are very hard particles they additionally score surfaces in relative contact, thus significantly increasing wear rate. It can be concluded that abrasive wear was dominant up to 10 m in case of 500 mN.

On the other hand, separation of surfaces in contact that happens due to accumulated wear debris should contribute in the opposite way to wear process. Dong and Bell [11] proved that Ti alloy oxides (e.g. TiO_2) are also produced on Ti alloy surface, related to oxidation process of Ti alloy and that they inhibit the wear process. Some authors [15,16] suggested that TiO_2 oxide generated on the Ti alloy surface has important role because it significantly lowers wear rate, while others suggested that it is of no such importance [14]. Accumulated wear debris did not produce lowering of the wear rate, for conditions in our study (250 mN, 500 mN, 750 mN), but increased it, indicating third-body abrasion. Regions with rusted appearance throughout the wear tracks (denoted by TH in Fig. 3) most probably indicated that tribochemical reactions occurred during sliding. Tribochemical reactions were always present, and noticed, under all test conditions, using visual observation of the samples just after the testing was finished. Later it was also confirmed with OM of cleaned wear track, as the change of the color in some regions of the wear track, as shown in Fig. 3 (TH). It most probably influenced tribological processes of surfaces in contact.

These complex phenomena occurring during reciprocating sliding of Ti6Al4V alloy against alumina has been studied by number of authors from different aspects [11–14,17,22]. It is in accordance with the trend of the wear factor curve in Fig. 7b, indicating complex wear behaviour. Difference of k and k_{PD} results shown in Fig. 6, is also in accordance with these findings, because calculation of wear factor according to ASTM G133 does not consider wear debris influence.

The highest applied load (1000 mN) produced fine wear debris in much smaller quantities. Some authors [11,12], proved that under the high loads, plastic flow of the surface layers of the Ti alloy occurs and begins to govern the wear behaviour together with mild adhesive wear due to rise in temperature within a contact zone. Number of authors [11,14,18–20], have studied influence of the high flash temperatures at asperities contact, that can be expected during sliding of the Ti alloy under a high load (up to 350 °C for experimental conditions within our study) or high sliding speeds. High load or high speed generates high flash temperatures. Due to temperature rise, Ti6Al4V alloy exhibit significant reduction in tensile strength, compressive and shear strength and elastic modulus [18]. Accordingly, material softening within the interface zone occurs and influences extensive plastic deformation and mechanical alloying of the materials in contact and favor plowing, galling and friction welding processes at asperities contact, further promoting adhesive wear mechanism. Plastic deformation of surface layers significantly influences tribological behaviour of the contact pair, by lowering wear rate. Wear factors that were obtained within our study for the highest normal load is in consistence with these findings.

It is likely that tribochemical mechanism has a more prominent role in case of low loads applied in our study, what is in consistence with conclusions of other authors [11,12,14]. In case of higher loads (250 mN, 500 mN, 750 mN), abrasive wear dominated with major influence of third-body abrasion by hard worn particles. In case of the highest load applied, low wear factors obtained here could be explained by occurrence of the plastic flow.

5. Conclusions

The following observations and conclusions were obtained.

1. According to observed results, it is possible to continuously monitor wear process by penetration depth parameter, recorded continuously by the tribometer. PD curves are related to development of the sample wear behaviour over time. PD parameter can be effectively used as additional mean for determination of wear mechanisms, in combination with optical micrographs of worn tracks. It enables further determination of wear mechanism zones, by analysis of wear factor curves.
2. Load exhibited transition characteristic for all conditions and sliding speed showed transition only for some regimes and for other it had no significant influence on the wear factor.
3. Certain load and speed regimes should be avoided, considering the transition nature of load and speed influence, as well as high wear factor values obtained under some testing conditions applied in this study (250–750 mN load and 8 mm/s).

Acknowledgement

This study was financed by Ministry of Science and Technological Development, Serbia, project no. 35021.

References

[1] M. Masmoudi, M. Assoul, M. Wery, R. Abdelhedi, F. El Halouani, G. Monteil, Appl. Surf. Sci. 253 (2006) 2237–2243.
[2] M. Masmoudi, M. Assoul, M. Wery, R. Abdelhedi, F. El Halouani, G. Monteil:, J. Alloys Compd. 478 (2009) 726–730.
[3] P.S. Walker, G.W. Blunn, P.A. Lilley, J. Biomed. Mater. Res. Part B 33 (1996) 159–175.
[4] M. Long, Hj. Rack, Wear 205 (1997) 130–136.
[5] M. Meozzi, Tribol. Int. 39 (2006) 496–505.
[6] P. De Baets, F. Van De Velde, A.P. Van Peteghem, Wear 208 (1997) 50–56.
[7] J. Black, G. Hastings (Eds.), Handbook of Biomaterial Properties, Chapman & Hall, London, 1998.
[8] M. Geetha, A.K. Singh, R. Asokamani, A.K. Gogia, Prog. Mater. Sci. 54 (2009) 397–425.
[9] M.P. Gispert, A.P. Serro, R. Colaco, B. Saramango, Wear 260 (2006) 149–158.
[10] H. Czichos, T. Saito, L. Smith (Eds.), Handbook of Materials Measurement Methods, Springer, Berlin, 2006.
[11] H. Dong, T. Bell, Wear 225–229 (1999) 874–884.
[12] A. Molinari, G. Straffelini, B. Tesi, T. Bacci, Wear 208 (1997) 105–112.
[13] J. Qu, P.J. Blau, T.R. Watkins, O.B. Cavin, N.S. Kulkarni, Wear 258 (2005) 1348–1356.
[14] M Long, H.J. Rack, Wear 249 (2001) 158–168.
[15] H. Hong, W.O. Winer, Trans. ASME J. Tribol. 111 (1989) 504–509.
[16] J.A. Davidson, Jpn. J. Tribol. 37 (1992) 399–413.

[17] I. Cvijovic-Alagic, S. Mitrovic, Z. Cvijovic, Dj. Veljovic, M. Babic, M. Rakin, Tribol. Ind. 31 (2009) 3–4.
[18] C.H. Hager Jr., J.H. Sanders, S. Sharma, Wear 260 (2006) 493–508.
[19] W.S. Lee, C.F. Lin, J. Mater. Process. Technol. 75 (1998) 127–136.
[20] A. Vairis, M. Frost, Mater. Sci. Eng. A 292 (2000) 8–17.
[21] M. Babic, S. Mitrovic, R. Ninkovic, Tribol. Ind. 31 (2009) 1–2.
[22] I. Cvijovic-Alagic, Z. Cvijovic, S. Mitrovic, M. Rakin, Dj. Veljovic, M. Babic, Tribol. Lett. 40 (2010) 59–70.